www.czasopisma.pan.pl PAN POLSKA AKADEMIA NAUK www.journals.pan.pl

Arch. Metall. Mater. **63** (2018), 2, 589-596

DOI: 10.24425/118978

A. CWUDZIŃSKI*#

NUMERICAL AND PHYSICAL MODELING OF LIQUID STEEL BEHAVIOUR IN ONE STRAND TUNDISH WITH GAS PERMEABLE BARRIER

The object of investigation was the one-strand tundish with flow control device such as gas permeable barrier (GPB). The aim of this flow control device was to activate the motion of liquid steel in the tundish longitudinal axis region. Computer simulation of the liquid steel flow and argon behaviour in isothermal turbulent motion conditions was done using the Ansys-Fluent computer program. For the validation of the hydrodynamic patterns obtained from computer simulations, a isothermal tundish glass model was used. Tundish glass model enables the recording of the visualization of fluid medium motion through the particle image velocimetry (PIV) method. Based on computer simulations, the liquid steel flow path lines in the tundish with GPB was obtained. For explain the hydrodynamic phenomena occurring in the tundish working space, the Buoyancy number has been calculated.

Keywords: tundish, gas permeable barrier, hydrodynamic conditions, numerical and physical simulations

1. Introduction

Continuous steel casting (CSC) enables the flexible production of slabs, blooms and billets. Casting of slabs, blooms or billets with varying chemical composition in the same casting sequence requires advanced ladle treatment and an optimized strategy for planning successive heats in the steelmaking furnace. One of the key elements determining the quality of slabs, blooms or billets is the quantity and distribution of non-metallic inclusions (NMI) occurring within their volume. A smaller quantity of non-metallic inclusions or their reduced size allow the manufacture of finished products to be operated under non-standard temperature or pressure conditions. Therefore, improving the CSC technology in terms of maintaining the required steel purity is justifiable. In order to select the optimal technological solution for the CSC process, tools in the form of numerical or physical models reflecting industrial conditions and industrial measurements are used [1-7]. Operations aiding the refinement of steel can be effectively performed in the tundish. The tundish ensures the stable and uniform feed of steel to the primary cooling zone, where the slabs, blooms or billets is formed and shell forms. The residence of steel for a specific time in the tundish allows it to be further treated to additionally remove the non-metallic inclusions. For this purpose, various devices are used to control the steel motion and intensify the process of non-metallic inclusion flotation towards the slag phase [8-13]. Examples of such devices are gas-permeable barriers (GPB) [13-21]. Having the form of a dam furnished with a gas-permeable shaped piece, these devices enable the change of the steel motion direction and NMI removal to the tundish slag. Gas permeable barrier also affect on hydrogen, oxygen and nitrogen content and horizontal velocity of liquid steel, both amount of gases and magnitude velocity decreased [22-23]. However argon injection system has some disadvantages i.e.: gas bubbles remove the flux from free surface of liquid steel, stimulate entrainment of tundish powder particles, wear tundish refractory and decrease liquid steel temperature [22]. Gas permeable barriers should generated bubbles in the dimension range between 1 and 5 mm in relation to the best interaction bubbles with non-metallic inclusions [24-28]. Moreover porous material in the gas permeable barrier cause formation of large number of bubbles with high possibility of coalescence and low possibility of break-up [29-30]. Therefore technology of argon injection in the tundish required inter alia suitable porous material, argon flow rate, chemical composition of tundish powder, balance of heat transfer and correlation with continuous casting steel grades. Based on the results of studies [31-34] it has been found that, in the single-nozzle wedge-type tundish, the best results in terms of steel motion optimization and expected refinement results are obtained for the GPB positioned on the mid-length of the bottom and low dam location in the tundish filling zone and for argon flow rate at a level of 10 and 20 Nl/min. On the other hand, study [35] has found that, in the facility (tundish without GPB) under consideration, the feed streams move along the side walls as they flow to the tundish nozzle; therefore, it is necessary to activate the steel motion in the tundish longitudinal axis region without changing behavior

* CZESTOCHOWA UNIVERSITY OF TECHNOLOGY, FACULTY OF PRODUCTION ENGINEERING AND MATERIALS TECHNOLOGY, DEPARTMENT OF METALS EXTRACTION AND RECIRCULATION, 19 ARMII KRAJOWEJ AVE, 42-200 CZESTOCHOWA, POLAND

Corresponding author: cwudzinski@wip.pcz.pl

of mean feed streams. The study has presented a new type of gas-permeable barrier for a single-nozzle wedge-type tundish and the results of numerical and physical simulation of liquid steel and water behavior.

2. Research methodology

2.1. Tundish with gas permeable barrier

The object of investigation was the one-strand tundish with stopper rod system and low dam [31]. Figure 1 shows a picture of the virtual model with new type of gas permeable barrier (GPB) and the marked location of bubbles active surface introducing the argon to the liquid steel (Fig. 1a) and a physical model of tundish (Fig. 1b). The tundish was equipped with a gas permeable barrier with a 0.75 × 0.05 m injection surface (bubbles active surface). In the GPB region contacting the longitudinal tundish walls, the GPB surface was made of a gas impermeable material. The aim of this design operation was to activate the motion of liquid steel and reduction of affect range of back flow streams in the tundish longitudinal axis region and protect feed streams, which occurs at the longitudinal walls of a tundish with no argon injection system.

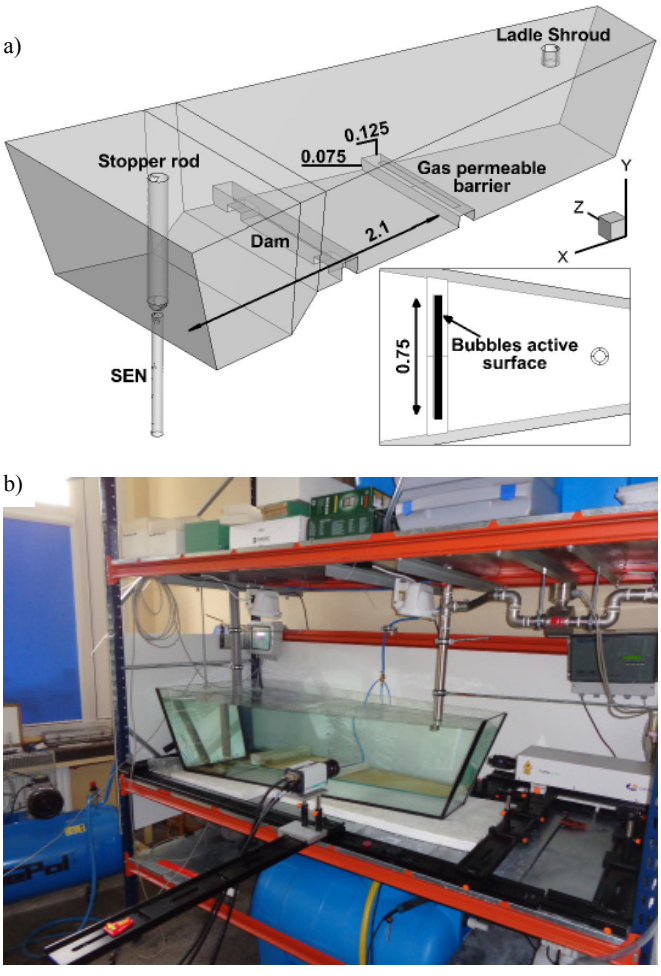

Fig. 1. One strand tundish: a) virtual model with position of gas permeable barrier, b) laboratory stand – physical model

2.2. Water model

For the validation of the hydrodynamic patterns obtained from computer simulations, describing the behaviour of the liquid steel, a physical tundish model was used [35]. The isothermal glass tundish model was made in a scale of 1:2.5 and enables the recording of the visualization of fluid medium motion through the particle image velocimetry (PIV) method. The 0.4 scale water model not allow obtain conformity of Reynolds criterion which describe ratio of inertial to viscous forces between industrial tundish and water model. Therefore velocity magnitudes of liquid steel and water will be different. However adopted water model were conducted while satisfying the Froude criterion, which ensured that the similarity between the inertial forces and the gravity forces occurring in the physical model and those prevailing in the metallurgical plant was maintained. This fact enable obtaining in the laboratory scale views of flow reflecting real directions of liquid steel flow by smaller velocity magnitudes of fluid. Especially, that for isothermal water model changing in the values of Reynolds number (by variation of water flow rate inlet) not affect on characteristic flow pattern [36]. The basic expression describing the initial volumetric flow rate of water and air in the physical model under examination is as follows:

$$Q_w = \lambda^{2.5} Q_{ls} \tag{1}$$

where: Q_w – water volumetric flow rate m^3/s, Q_{ls} – liquid steel volumetric flow rate m^3/s, λ – scale factor.

Air at a flow rate of 1 Nl/min was blown into the physical tundish model through a specially designed GPB. In spite of appearance of difference in behaviour of air bubbles in the water and argon bubbles in the liquid steel both systems show similar tendency [37]. Therefore air-water system can be successfully using to laboratory trials. Within the conducted project, the physical tundish model was additionally equipped with a double frame sCMOS camera for recording water behaviour in zone of air bubbling. Camera and a double-cavity laser of a pulse energy of 200 mJ and a wavelength of 532 nm with an optical light knife system with a light beam propagation angle from 15° to 30° was used during laboratory trials. For the analysis of the vector flow field the DaVis 8.0 software program with the 2DPIV module was employed. Seeding in the form of 5 mL glass balls of a density of 1100 kg/m^3 (±50 kg/m^3) and an average diameter from 9 to 13 μm was introduced to the water flowing through the tundish model. The measurement of water flow field in the physical model was started after a period of four average water residence time, which means casting one heat. This time allows obtain steady conditions in the physical glass model. During a single measurement, 99 double frames were recorded, which provided a basis for obtaining the vector flow field. Time between frames was 0.02 second. The measurement was repeated 10 times at intervals of 5 minutes. In the next stage of analysis, the recorded glass ball motion was transformed into the vector field form using the 2DPIV module.

2.3. Numerical model

Computer simulation of the liquid steel flow and argon behaviour in isothermal turbulent motion conditions was done using the Ansys-Fluent® computer program. The basic mathematical model equations describing the phenomena under examination are as follows:

$$\frac{\partial \rho}{\partial t} + \nabla(\rho u) = 0 \tag{2}$$

$$\frac{\partial}{\partial t}(\rho u) + \nabla(\rho u u) = -\nabla p + \nabla(\bar{\bar{\tau}}) + \rho g \tag{3}$$

where: u – liquid steel velocity m/s, ρ – liquid steel density kg/m^3, t – time s, p – pressure Pa, g – gravitational acceleration m/s^2, $\bar{\bar{\tau}}$ – stress tensor Pa.

For describing the turbulence motion of liquid steel and argon realizable k-ε model was adopted. In the realizable k-ε turbulence model, constants take on the following values: C2 = 1.9, σk = 1.0, $\sigma \varepsilon$ = 1.2 [38]. To reproduce the process of argon blowing through the gas permeable barrier, a discrete phase model as described by equation no. 4 was used. The effects of the chaotic behavior of bubbles in the volume of liquid steel are described by the discrete random walk model (equation 5).

$$\frac{du_B}{dt} = \frac{18\mu C_D \,\mathrm{Re}}{24\rho_B d_B^2}(u - u_B) + \frac{g(\rho_B - \rho)}{\rho_B} + \frac{1}{2}\frac{\rho}{\rho_B}\frac{d(u - u_B)}{dt} \tag{4}$$

$$u_B^{'} = \zeta\sqrt{\frac{2k}{3}} \tag{5}$$

where: u_B – velocity of bubble m/s, C_D – drag coefficient, ρ_B – density of bubble kg/m^3, Re – Reynolds number, d_B – diameter of bubble m, $u_B^{'}$ – bubble random velocity fluctuation, m/s, k – kinetic energy of turbulence, m^2/s^2, ζ – random number.

The turbulence intensity (TI) of liquid steel was expressed by equation 6:

$$TI = \frac{\sqrt{\frac{2}{3}k}}{u} \tag{6}$$

At the tundish inlet (initial boundary condition), a liquid steel inflow of 1.316 m/s was assumed with turbulence kinetic energy 0.0173 m^2/s^2 and energy of dissipation rate of kinetic energy 0.065137 m^2/s^3. The liquid steel properties are as follows: density, 7010 kg/m^3; viscosity, 0.007 Pa×s. Physical quantities of argon were as follows: density, 1.62 kg/m^3. During numerical simulation argon at a flow rate of 10 Nl/min was blown into the liquid steel through a GPB. 1 mm-diameter spherical bubbles were blown into the liquid steel. The initial boundary condition for liquid steel at the tundish inlet was the same like in the previous author's work [35]. The free steel table surface was described using the boundary condition of a wall with zero stresses. The virtual object was built of tetrahedral elements. All numerical simulations were done by employing a double-precision solver (3ddp) using discretization of the second order. For describing the velocity and pressure fields, the Semi-Implicit Method for Pressure-Linked Equation-Consistent algorithm was selected. Computer simulations and laboratory experiments of liquid steel/water and argon/air behaviour were performed for the sequence of casting 1.5 m × 0.225 m slabs at a speed of 0.9 m/min and for steady conditions.

3. Results and discussion

3.1. Model validation

Based on computer simulations and laboratory experiments, the picture of steel behaviour in the tundish with GPB was obtained. The first stage of the investigation included the verification of flow steel results obtained from computer simulations by comparing them with the motion of water recorded in the physical model and calculated by the PIV method. Figure 2 shows the liquid steel and water motions in the tundish longitudinal axis region. In Figure 2a, the region chosen for the analysis of numerical simulation and laboratory experiment results is indicated. The steel motion (numerical simulation) in the measurement region is dominated by reverse streams flowing towards the feed stream and the tundish bottom (Fig. 2a). Under the liquid steel free surface, being arranged horizontally, the streams reach the ladle shroud region. In contrast, with increasing distance from the free surface, the steel streams start forming into vertical patterns as they fall down towards the tundish bottom. Figures 2b-f show the motion of water in the tundish physical model. Like for liquid steel, also the motion of water in the measurement region is dominated by reverse streams, which change their arrangement from horizontal to vertical as they approach the pouring zone, flowing towards the tundish bottom. The water motion fields recorded during laboratory experiments show the effect of the tundish feeding stream, which, flowing in the opposite direction, influences the reverse streams occurring in that part of the tundish. Moreover, the water motion fields, obtained by the PIV method, are characterized by a periodical differentiation in the picture of the hydrodynamic pattern. The periodical water motion modifications in the form of variations in the distribution of horizontal and vertical streams and the occurrence of water recirculation at the free surface provide important information on the dynamics of the hydrodynamic patterns forming in the tundish working space during the continuous casting process. Laboratory experiments have confirmed that the employed numerical model adequately reflects the steel motion in relation to directions of streams flow in the gas-permeable barrier tundish.

3.2. Liquid steel motion

The second stage of the investigation involved the description of steel flow within the whole working space of the tundish with new type of gas permeable barriers. Figure 3 shows the results for the behaviour of liquid steel and argon in the longitu-

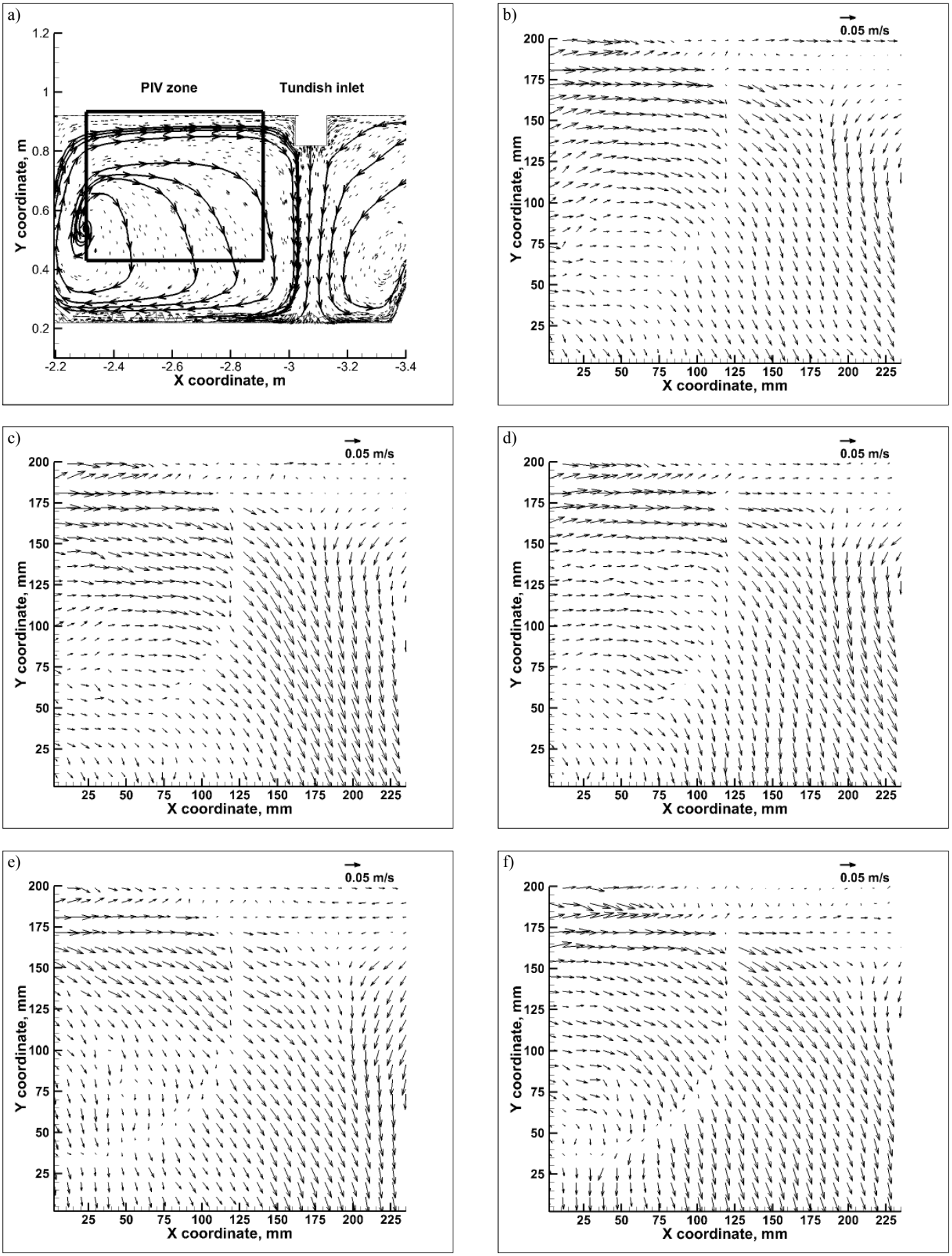

Fig. 2. Flow fields: a) numerical liquid steel flow, b) physical liquid water flow – trial no. 1, c) physical liquid water flow – trial no. 2, c) physical liquid water flow – trial no. 3, d) physical liquid water flow – trial no. 4, e) physical liquid water flow – trial no. 5

dinal axis region in the plane covering the tundish pouring zone, affected by the gas-permeable barrier and the stopper rod system. After flowing into the tundish, the stream undergoes disintegration into mould feed streams, reverse streams and circulating streams (Fig. 3a). Having passed through the gas-permeable barrier zone, the mould feed streams gradually fall towards the nozzle. At the same time, a circulation zone forms between the conventional dam and the gas-permeable barrier, from which part of the streams turn into reverse streams. The motion of argon towards the free surface causes a steel circulation region to form also at the pouring zone. The third stream circulation zone occurs between the feed stream and the rear transverse tundish wall. Introducing argon to the steel results in accelerating the steel motion in the gas-permeable barrier-affected zone up to a value of 0.1 m/s (Fig. 3b). For this reason, the gas-permeable barrier constitutes, besides the feed stream, the second source of driving force responsible for the intensity of mass transfer within the tundish working space. The intensity of steel turbulence in the zone of blowing argon at a flow rate of 10 Nl/min does not exceed 0.05. Similar values of turbulence intensity were recorded in the tundish pouring zone near tundish bottom and walls (Fig. 3c). The difference between argon and liquid steel in specific density causes introduced bubbles to quickly flow out from the steel to head for the free surface (Fig. 3d). Thus, the argon bubbles effectively influence the liquid steel motion. The interaction of argon bubbles with liquid steel translates into a specific steel motion in the tundish working space.

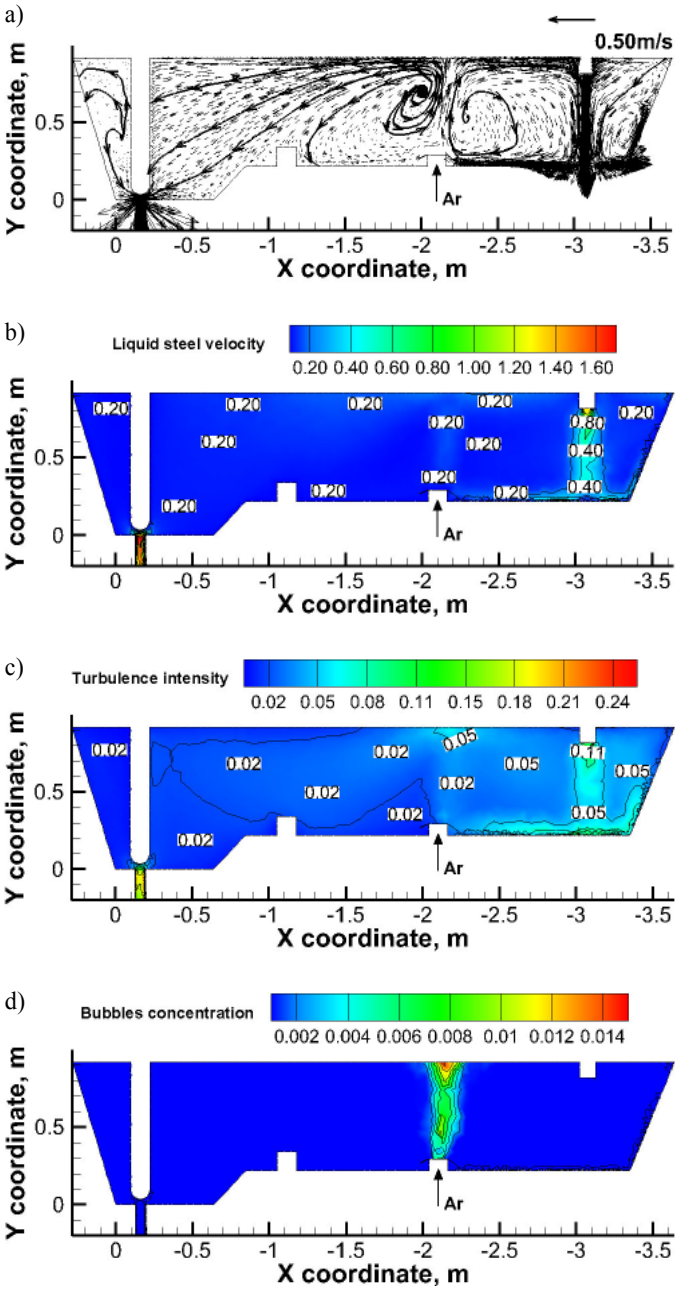

Fig. 3. Numerical results for the tundish longitudinal axis region: a) liquid steel flow direction (m/s), b) liquid steel velocity (m/s), c) liquid steel turbulence intensity (-), d) argon concentration (-)

3.3. Liquid steel path lines

For better understanding advantages of using argon injection system Figure 4a shows the motion paths of the liquid steel streams occurring in the tundish without GPB. In the tundish longitudinal axis region, the flow has a descending pattern and takes place in a vertical configuration. The flow pattern looks as follows: the main feeding stream, after flowing to the tundish, continues towards the bottom and then to the lateral walls of the

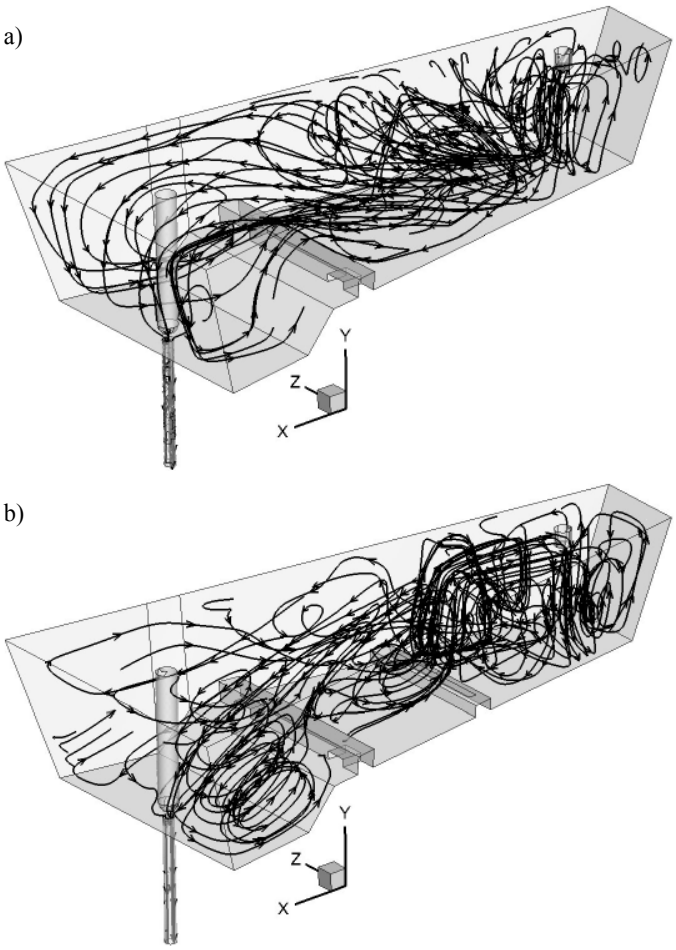

Fig. 4. Complete liquid steel path lines: a) tundish with low dam, b) tundish with low dam and gas permeable barrier

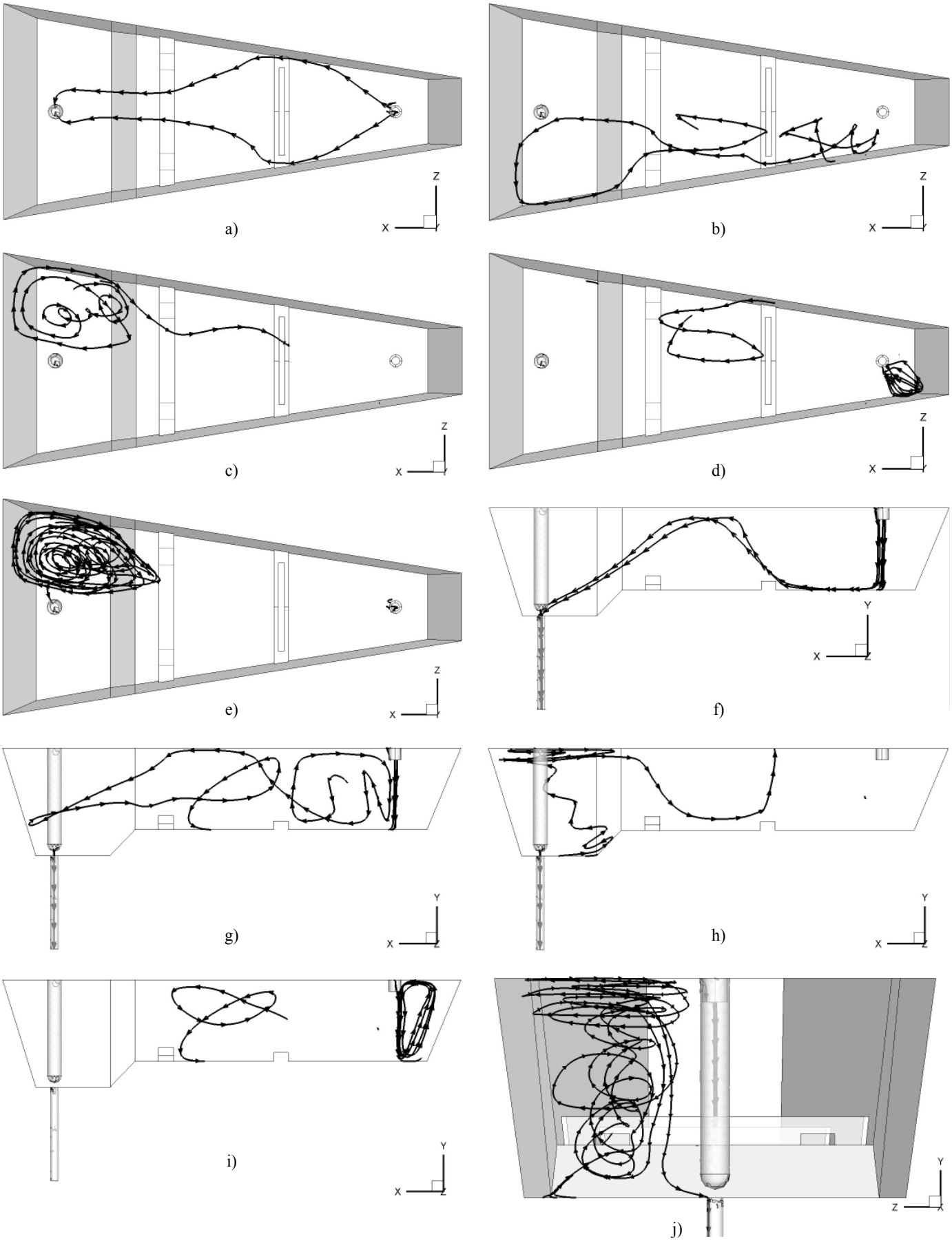

Fig. 5. Local liquid steel path lines: a) streams flow to SEN – top view, b) backflow stream – top view, c) circulating and backflow stream – top view, d) recirculation stream – top view, e) rotary streams – top view, f) streams flow to SEN – side view, g) backflow stream – side view, h) circulating and backflow stream – side view, i) recirculation streams – side view, j) rotary streams – side view

tundish. Part of the liquid steel in the pouring zone starts circulating, while the remaining part of the liquid steel flows towards the free steel surface and up to the stopper rod system zone. After reaching the stopper rod system zone, liquid steel streams start to circulate within a region situated between tundish bottom and free steel surface. Next, the liquid steel flows towards the outlet. Some liquid steel streams flow to pouring zone create back flow streams. Figure 4b shows complete path lines of liquid steel for tundish with gas permeable barrier. Three characteristic liquid steel flow zones can be distinguished in this figure, namely a strong horizontal and vertical recirculation streams zone in the region between pouring zone and GPB, a steel circulation zone located between GPB and low dam and a descending and recirculation streams zone in the stopper rod system region. In order to systematize the liquid steel motion directions recorded in the tundish working volume with GPB Figure 5 illustrates a detailed hydrodynamic analysis. The motion of steel is largely symmetrical with relative to the axis intersecting the tundish lengthwise (Fig. 5a and 5f). After flowing into the tundish, the mould feed streams hit the bottom and then move along the bottom towards the longitudinal walls, and then go past the gas-permeable barrier at the location, where the argon blow-in zone is inactive. Next, heading for the nozzle, the streams flow towards the free surface, more and more closely approaching the central part of the tundish working space (Fig. 5a and 5f). Reverse streams, on the other hand, may have their origin either in the zone between the gas-permeable barrier and the pouring zone (Fig. 5b and 5g) or in the immediate vicinity of the stopper rod system zone (Fig. 5c and 5h). Part of streams formed by argon bubbles introduced to the liquid steel may also circulate in the zone between the gas-permeable barrier and the conventional dam (Fig. 5d and 5i). In the tundish pouring zone, the streams formed from the disintegration of the feed stream may also circulate from the bottom towards the free surface between the longitudinal walls and the rear transverse wall (Fig. 5d and 5i). The nozzle feed stream motion orientation towards the central tundish part, shown in Figure 5a, is the result of the steel circulation region occurring in the stopper rod system zone (Fig. 5e and 5j). The liquid steel rotational motion changes from vertical to horizontal motion. From the rotational motion zone on, part of the streams flows to the SEN (Fig. 5j), and the other part penetrates through the working spaces of the tundish (Fig. 5c).

3.4. Influence of natural convection

For tundishes, an important factor also determining the hydrodynamic pattern is the natural convection caused by temperature gradients and velocities attained by steel streams [39-42]. The reported results of computer simulations and laboratory experiments refer to isothermal casting conditions, which are very hard to achieve in industrial practice. For this reason, the average value of liquid steel velocity (u = 0.046 m/s) for the facility under examination was red out, and then it was verified for which temperature gradient value an additional modification of the steel motion, caused by natural convection forces, could be expected. Therefore to explain the phenomena occurring in the tundish working space, the Buoyancy number (Bu), as described by equation 7 has been calculated.

$$Bu = \frac{g\beta\Delta TL}{u_{avg}^{2}} \tag{7}$$

The Buoyancy (Bu) number describes the effect of natural convection of modifying the fluid flow pattern, and expresses the ratio of buoyancy forces to inertial forces occurring in the system. A Bu number value above 5 means that the liquid metal flowing through the tundish will be affected by natural convection. Figure 6 illustrates the dependence of the Bu number on the temperature gradient. For the facility under analysis, the mean maximum temperature gradient, being the difference in temperature between the liquid steels flowing to and out of the tundish, is 4÷5 K [43]. By analysing different values of the temperature gradient it was found that, for the tundish equipment variant under investigation and an argon blow-in rate of 10 Nl/min, non-isothermal conditions should not significantly influence the steel motion modification. This is indicated by the value of the Bu number which, for the temperature gradient at a level of 9 K and a maximum depth of 0.92 m, is to 3.83. Blown-in argon influences the motion of steel, making the inertia forces generated by the feed stream and argon bubbles decisive factors influencing the steel motion in the facility under examination.

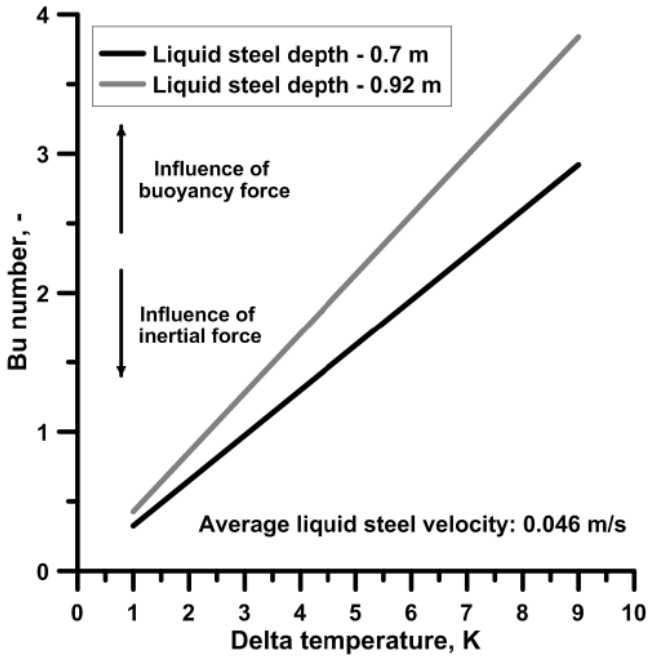

Fig. 6. Influence of delta temperature on buoyancy force

4. Summary

From the performed computer simulations and laboratory trials it can be found that:

- The directions of water flow in the physical model confirm the behaviour of liquid steel shown in computer simula-

tions. In both cases, reverse streams descending towards the facility's bottom occurred in the examined region.

- The use of the new type of gas-permeable barrier results in the effective activation of steel motion in the tundish longitudinal axis region, causing streams recirculation on either side of the gas permeable barrier.
- Introducing argon to the steel increases the velocity of liquid steel flow through the tundish working space. Therefore, a decisive factor influencing the hydrodynamic pattern in the facility under analysis will be inertia forces generated by the feed stream and gas bubbles moving within the injection region.

Acknowledgements

The research work has been financed from the Ministry of Science and Higher Education resources as IuventusPlus programme in the years 2015-2016 project no. IP2014 006973

REFERENCES

[1] M. Janik, H. Dyja, J. Mater. Process. Tech. **157-158**, 177-182 (2004).
[2] H. Zhang, W. Wang, F. Ma, L. Zhou, Metall. Mater. Trans. B. **46**, 2361-2373 (2015).
[3] K. Miłkowska-Piszczek, J. Falkus, Metalurgija **53**, 571-573 (2014).
[4] R. Pyszko, M. Příhoda, P. Fojtík, M. Kováč, Metalurgija **51**, 149-152 (2012).
[5] J.J.M. Peixoto, W.V. Gabriel, L.Q. Ribeiro, C.A. da Silva, I.A. da Silva, V. Seshadri, J. Mater. Process. Tech. **233**, 89-99 (2016).
[6] K. Jin, B.G. Thomas, X. Ruan, Metall. Mater. Trans. B **47**, 548-565 (2016).
[7] I. Calderon-Ramos, R.D. Morales, Metall. Mater. Trans. B **47**, 1866-1881 (2016).
[8] Y. Miki, B.G. Thomas, Metall. Mater. Trans. B **30**, 639-654 (1999).
[9] L. Zhang, S. Taniguchi, K. Cai, Metall. Mater. Trans. B **31**, 253-266 (2000).
[10] M. Warzecha, T. Merder, P. Warzecha, G. Stradomski, ISIJ Int. **53**, 1983-1992 (2013).
[11] H. Ling, L. Zhang, JOM **65**, 1155-1163 (2013).
[12] C. Chen, P. Ni, L.T.I. Jonsson, A. Tilliander, G. Cheng, P.G. Jönsson, Metall. Mater. Trans. B **47**, 1916-1932 (2016).
[13] D. Chen, X. Xie, M. Long, M. Zhang, L. Zhang, Q. Liao, Metall. Mater. Trans. B. **45**, 392-398 (2014).
[14] A. Vargas-Zamora, R.D. Morales, M. Díaz-Cruz, J. Palafox-Ramos, J. De J. Barreto-Sandoval, Metall. Mater. Trans. B. **35**, 247-257 (2004).
[15] C. Cicuttin, A. Martin, J. Mendez, M. Romero, G. Di Gresia, Proceed. 7th European Continuous Casting Conf. 1-10, Düsseldorf 2011.
[16] D. Janssen, J. Simoes, P. Desai, Proceed. 7th European Continuous Casting Conf. 1-8, Düsseldorf 2011.
[17] A.N. Smirnov, V.G. Efimova, A.V. Kravchenko, Steel in Transl. **43**, 673-677 (2013).
[18] R. Ehrengruber, Proceed. 8th European Continuous Casting Conf. 1080-1091, Graz 2014.
[19] D. Chatterjee, J. Inst. Eng. India Ser. D. DOI 10.1007/s40033-015-0093-5 (in press).
[20] R.D. Morales, A. Ramos-Banderas, R. Sanchez-Perez, AISTech Proceed. **2**, 867-877, Nashville 2004.
[21] L. Zhong, L. Li, B. Wang, M. Jiang, L. Zhu, R. Che, Steel Res. Int. **77**, 103-106 (2006).
[22] Y. Sahai, T. Emi, Tundish technology for clean steel production, 2008 World Scientific.
[23] G. Stolte, Secondary metallurgy, 2002 Verlag Stahleisen GmbH.
[24] M. Guy, I. de Poloni, P. Blostein, M. Devaux, Proceed. 1st European Continuous Casting Conf. 193-202, Florence 1991.
[25] L. Zhang, S. Taniguchi, ISS Trans. 55-79 (2001).
[26] L. Zhang, B. G. Thomas, J. Univ. Scien. and Tech. Beijing. **13**, 293-300 (2006).
[27] R. Moravec, L. Valek, J. Pys, Proceed. SteelSIM Conf. 107-114, Brno 2005.
[28] L. Wang, H.-G. Lee, P. Hayes, ISIJ Int. **36**, 7-16 (1996).
[29] P. E. Anagbo, J.K. Brimacombe, Metall. Mater. Trans. B **21**, 637-648 (1990).
[30] A. Alexiadis, P. Gardin, J.F. Domgin, Metall. Mater. Trans. B **35**, 949-956 (2004).
[31] A. Cwudziński, Steel Res. Int. **81**, 123-131 (2010).
[32] A. Cwudziński, Canad. Metall. Quart. **49**, 63-72 (2010).
[33] A. Cwudziński, Ironmak. Steelmak. **37**, 169-180 (2010).
[34] A. Cwudziński, Arch. Metall. Mater. **56**, 611-618 (2011).
[35] A. Cwudziński, Steel Res. Int. **86**, 972-983 (2015).
[36] H.J. Odenthal, H. Pfeifer, M. Klaas, Steel Res. Int. **71**, 211-219 (2000).
[37] H. Bai H., B.G. Thomas, Metall. Mater. Trans. B. **32**, 1143-1159 (2001).
[38] T.-H. Shih, W. W. Liou, A. Shabbir, Z. Yang, J. Zhu, Comput. Fluid. **24**, 227-238 (1995).
[39] A. Vargas-Zamora, R.D. Morales, M. Diaz-Cruz, J. Palafox-Ramos, L. Garcia Demedices, Int. J. Heat Mass Transf. **46**, 3029-3039 (2003).
[40] H.J. Odenthal, R. Bolling, H. Pfeifer, Steel Res. Int. **74**, 44-55 (2003).
[41] D. Y. Sheng, C. S. Kim, J. K. Yoon, T. C. Hsiao, ISIJ Int. **38**, 843-851 (1998).
[42] R.I.L. Guthrie, M. Isac, I&SM. 27-32 (2003).
[43] A. Cwudziński, J. Jowsa, Metall. Found. Eng. **33**, 97-103 (2007).